





# Impact of temperature, bed height, and particle size on Ni(II) removal in a continuous system: Modelling the break curve

Angel Villabona-Ortíz<sup>1)</sup> , Candelaria Tejada-Tovar<sup>1)</sup> , Rodrigo Ortega-Toro<sup>2)</sup> ,  
Keily Peña-Romero<sup>1)</sup> , Ciro Botello-Urbiñez<sup>1)</sup>

<sup>1)</sup> Universidad de Cartagena, Department of Chemical Engineering, Cartagena de Indias, Colombia

<sup>2)</sup> Universidad de Cartagena, Department of Food Engineering, Carrera 6, Cl. de la Universidad 36-100, Cartagena de Indias, Colombia

RECEIVED 25.11.2020

REVIEWED 21.01.2021

ACCEPTED 28.06.2021

**Abstract:** The objective of this research was to evaluate the adsorption capacity of the shell biomass (*Dioscorea rotundata*), taking into account the impact of temperature, bed height, and particle size on the removal of nickel(II) ions in aqueous solution in a continuous fixed-bed column system; performing the modelling of the break curve. The biomass was characterised by SEM-EDS analysis. The analysis found that it represents a rough, heterogeneous structure, rich in carbon and oxygen, with mesopores, and is suitable for removing heavy metals. It also determined the optimum parameters of the bed height, particle size, and temperature, keeping the pH and the initial concentration of the solution constant. The results revealed that the bed height and the particle size are the two most influential variables in the process. Ni(II) removal efficiencies range between 85.8 and 98.43%. It was found that the optimal conditions to maximise the efficiency of the process are temperature of 70°C, 1.22 mm particle size, and 124 mm bed height. The break curve was evaluated by fitting the experimental data to the Thomas, Adams–Bohart, Dose–Response, and Yoon–Nelson models, with the Dose–Response model showing the best affinity with a coefficient of determination  $R^2$  of 0.9996. The results obtained in this research showed that yam shell could be suggested as an alternative for use in the removal of Ni(II) ions present in an aqueous solution in a continuous system.

**Keywords:** bio-sorption, Dose–Response model, packed bed, Thomas model

## INTRODUCTION

Population growth and industrial development have caused adverse environmental effects due to a large amount of pollutants discharged into water sources [NITHYA, *et al.* 2020; LIANG *et al.* 2017]. Among these pollutants, heavy metals, such as chromium, mercury, cobalt, nickel, lead, and arsenic, are poured into aquatic media as a result of processes such as mining, tanning, battery manufacturing, paint production, and other industrial activities [MOINO *et al.* 2017; WU *et al.* 2021]; they have a severe impact on humans, animals, and aquatic life, because of their stable nature, and resistance to degradation [BABARINDE *et al.* 2016; RESKE *et al.* 2020]. Nickel is a metal used in electroplating, metallisation, crude oil extraction processes, manufacturing of paint and powder, batteries, alloy, brass, and, everyday products such as cosmetics,

clothing, and electronics [HERRERA-BARROS *et al.* 2020; PRIYANTHA *et al.* 2019]. Several technologies, including membrane filtration, ion exchange, electrochemical techniques, and chemical precipitation have been proposed to remove nickel and other heavy metal ions from the aqueous solution [MAHARANA *et al.* 2021; YU *et al.* 2021]. The adsorption technique has been recognised as an attractive alternative to other contaminant removal techniques due to its easy handling, low cost, and availability of the adsorbents [BATOOL *et al.* 2018; SABIR *et al.* 2021].

In the adsorption of Ni(II), it has been employed in a continuous system, with the sugar cane bagasse achieving a removal rate of no more than 36.4% [ANOOP KRISHNAN *et al.* 2011], while passion fruit and grapefruit husks and bagasse achieved the maximum removal capacities in the bed for each bio-adsorbent amounting to 70.2, 29.1, and 12.1 mg·g<sup>-1</sup>,

respectively [CHAO *et al.* 2014]. Other experiments evaluated the removal of heavy metals with *Sargassum* sp. [BARQUILHA *et al.* 2017], reaching a removal rate of 1.23 mmol·g<sup>-1</sup> for nickel(II) and 1.51 mmol·g<sup>-1</sup> for copper(II); with cocoa shell [LARA *et al.* 2016], while 91.32% and 87.8% removal rates were achieved for lead(II) and copper(II), respectively. A wide variety of biomaterials have been studied to prepare adsorbents with suitable properties to absorb heavy metal ions. Food waste biomass is an attractive source of biomaterials that mitigate municipal solid waste disposal problems [MALIK *et al.* 2021]. Waste disposal on the northern coast of Colombia represents a severe problem for the environment and public health because agriculture has a significant impact on the total volume of solid waste generation, and dispersed agricultural sources contribute 84% of the biochemical oxygen demand of surface waters [BIGDELOO *et al.* 2021; TOBÓN-OROZCO, VASCO CORREA 2021]. In the northern region of Colombia, agricultural production focuses on yucca (*Manihot esculenta*) and yam (*Dioscorea rotundata*), which account for 35 and 18% of total production, respectively [TEJADA-TOVAR, *et al.* 2020].

Agricultural waste has been studied as an adsorbent for the removal of pollutants such as heavy metals [BISWAS, NAG 2021], nitrogen and phosphorus [DAI *et al.* 2018], dyes [AFROZE, SEN 2018], and organic pollutants [NAGHIZADEH *et al.* 2017]. In this study, agricultural crop biomass (*Dioscorea rotundata*), widely available in northern Colombia, is used to prepare the biosorbent and remove Ni(II) ions present in an aqueous solution. The optimal temperature, bed height, and particle size were evaluated in adsorption mode in a continuous system. The modelling of the break curve and the study of solute concentration in the solution over time were performed.

## MATERIALS AND METHODS

All reagents are analytical grade; nickel sulfate (NiSO<sub>4</sub>) was used to prepare the nickel solution at 100 mg·dm<sup>-3</sup>. HCl and 1 M NaOH were used to adjust the pH of the solution. Yam shells were collected as post-harvest waste. The best available biomass was selected, washed with deionised water, dried in a Lauda Alpha brand oven at 60°C for 24 hours, and reduced in size in a roller mill. The size classification was performed in a Shaker type sieve shaker, Edibon Orto Alresa brand, using sieves with mesh numbers 120, 45, 35, 18, and 16, according to the ASTM D6913-04 [2004], in order to select the sizes to evaluate 0.124, 0.355, 0.5, 1.0, and 1.19 mm. The bio-adsorbent was characterised, before and after adsorption, by scanning electron microscopy (SEM) and X-ray scattering (EDX).

### • Preparation of the adsorbent

The yam shell (*Dioscorea rotundata*) was obtained as postharvest waste from the Bolivar department area – Colombia. The shells that were in a good condition were selected, washed, dried in the sun until obtaining a constant mass, and reduced in size in a roller mill. After that, they were classified by size on a stainless steel sieve.

### • Adsorption tests

The adsorption experiments in a continuous packed bed system were performed following the experimental design, in adsorption equipment in acrylic columns of 25.64 cm in length and 4.4 cm in diameter [TEJADA-TOVAR *et al.* 2018]. The synthetic solution of Ni(II) with a concentration of 100 mg·dm<sup>-3</sup>, at pH 6,

and flow of 0.75 cm<sup>3</sup>·s<sup>-1</sup> was brought into contact with the adsorbent. An experimental design 2<sup>2</sup> in central star composite response surface was used for experimental development and carried out at Statgraphics Centurion. This type of design allows for studying the effect of independent variables on the response when varying them simultaneously, performing the least number of experiments possible, without the need for replications, since it maps a region of a response surface [DEMIREL, KAYAN 2012]. The temperature (30, 40, 55, 70, and 80°C), the particle size (0.124, 0.355, 0.5, 1.0, and 1.19 mm), and the bed height (6.13, 30.65, 100, and 123.8 mm) were varied.

The system temperature was controlled by a resistor connected to a PID controller with a pump for recirculation. The concentration of Ni(II) in the solution was determined by atomic absorption at 232 nm in a Buck Scientific model 210 VGP atomic absorption spectrophotometer [MANJULADEVI, *et al.* 2018]. Adsorption efficiency was determined by Equation (1):

$$\%R = \frac{C_0 - C_f}{C_i} 100 \quad (1)$$

where:  $C_0$  = the initial concentration evaluated (mg·dm<sup>-3</sup>),  $C_f$  = the final concentration of Ni(II) in the solution after the adsorption tests (mg·dm<sup>-3</sup>),  $C_i$  = initial concentration in the solution before the adsorption tests (mg·dm<sup>-3</sup>).

### • Construction and modelling of the break curve

Once the experiments were performed, the optimal condition to execute the metal adsorption break curve was determined to study the adsorbent's behavior during the time [MARTÍN-LARA *et al.* 2017]. The statistical analysis of the results was carried out by analysing variance ANOVA and response optimisation in the Statgraphics Centurion XVII software. The adsorption capacity of the column was determined using Equation (2) [APIRATIKUL, CHU 2021]:

$$q_j = \frac{C_{jf}Q}{1000m_s} t_s \left( 1 - \frac{C_{jout}}{C_{jf}} \right) dt \quad (2)$$

where:  $q_j$  = the concentration of the  $j$ -ion in the adsorbent (mmol·g<sup>-1</sup>),  $C_{jf}$  = the feed concentration of the  $j$ -ion in the liquid phase (mmol·dm<sup>-3</sup>),  $Q$  = the volumetric flow rate of the solution flowing through the column (cm<sup>3</sup>·min<sup>-1</sup>),  $m_s$  = the mass of the biomass with which the tower is packed (g),  $C_{jout}$  = the output concentration of the  $j$ -ion in the liquid phase (mmol·dm<sup>-3</sup>),  $t_s$  = the time of column saturation (min).

The experimental data of the rupture curve were adjusted to the theoretical models of Adams–Bohart, the Thomas, the Yoon–Nelson, and the Dose–Response model, with the objective to describe and analyse the behaviour of the column through graphs ( $C/C_i$ )- $t$ .

## RESULTS AND DISCUSSION

### BIOADSORBENT CHARACTERISATION

The morphology of the yam shell was observed by scanning electron microscopy (SEM) with x200 magnification before and after removing the Ni(II) ions. The micrographs and EDS spectrum are shown in Figure 1.

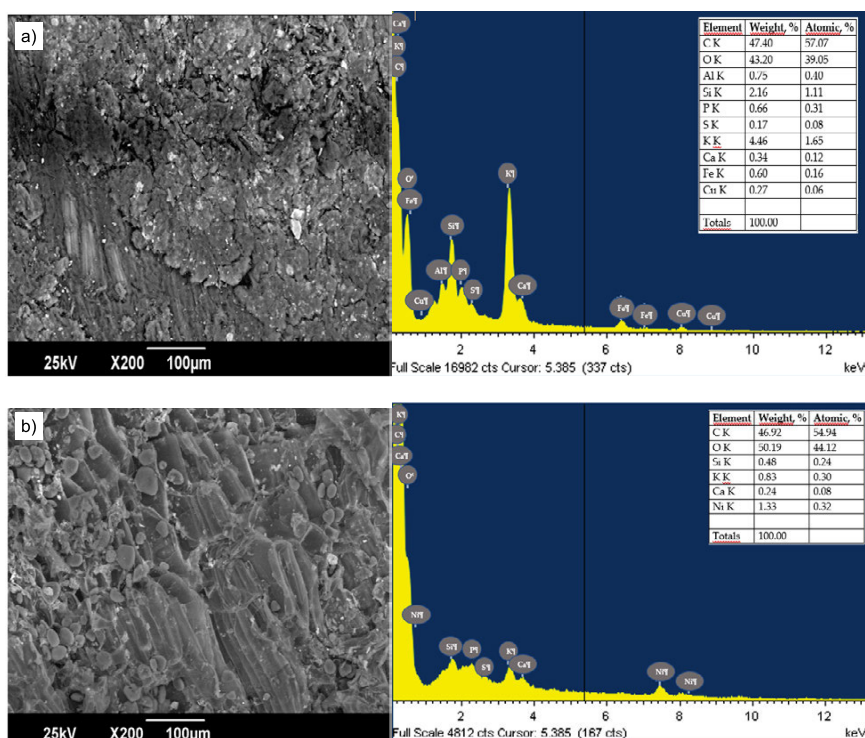


**Fig. 1.** SEM micrographs of the yam shell (a) before and (b) after Ni(II) adsorption; source: own study

It was observed that the surface of the biomass is irregular with the presence of mesopores [DENG *et al.* 2018]. From the EDS, it was established that the material presents a diverse structure, rich in oxygen, carbon, and calcium, with traces of multiple elements such as potassium, silicon, aluminum, phosphorus, and iron, among others. It has been reported that the presence of these materials attached to the functional groups of lignocellulosic materials is associated with the ability of this type of biomasses to capture ions through ion exchange [DENG *et al.* 2020]. After the adsorption process, the appearance of the Ni(II) ion in the EDS spectrum at the high-intensity peak 1.4 keV was observed; likewise, from the SEM micrography, it was evidenced that the exposed surface of the bio-adsorbent softens, which is attributed to the coating of the pores by the metallic ion [PRIYANTHA *et al.* 2019].

### ADSORPTION EXPERIMENTS

Figure 2 shows the effect of particle size, bed height, and temperature on Ni(II) removal efficiency, respectively. It was found that the best adsorption results were obtained at 1 mm size, 70°C temperature, and 124 mm bed height.

Figure 2a shows that adsorption efficiency increases in proportion to particle size in proportion to particle size. In batch system adsorption processes, it is common to find that the removal rate increases with the reduction of the particle diameter of the adsorbent, since it increases the surface contact area and the adsorbent's ability to capture contaminants [HERRERA-BARROS *et al.* 2020; RAULINO *et al.* 2014; SAADAT *et al.* 2016]. However, in a continuous bed system and the ideal particle size, the packed bed's tortuosity must be guaranteed to ensure contact of the contaminated solution with all the contaminants and thus maximise removal [TEJADA-TOVAR *et al.* 2018]. In the present

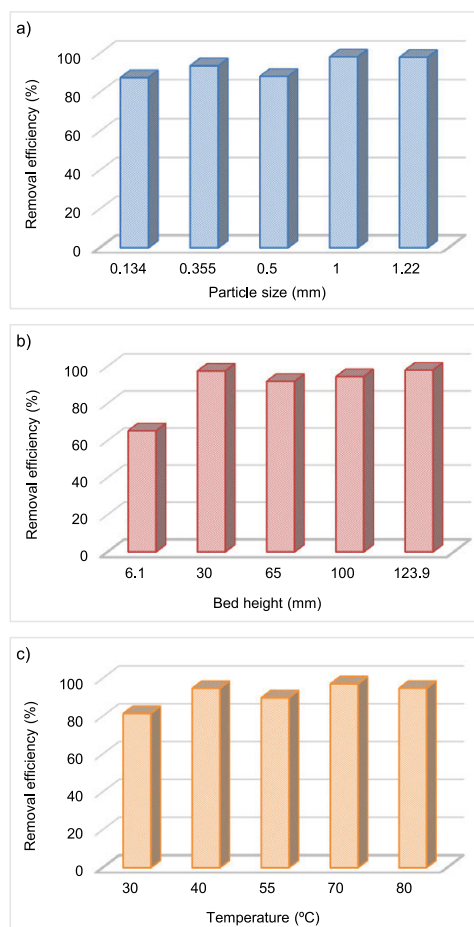


**Fig. 2.** Impact of a) particle size, b) bed height, c) temperature on Ni(II) removal efficiency; source: own study

study, it was found that increasing the particle size increases the percentage of Ni(II) ion removal, with this variable being the most influential in the process, according to the analysis of variance in Table 1. As regards the effect of the bed height reported in Figure 2b, it is observed with a bed height of 124 mm. The removal efficiency is maximum because the higher amount of adsorbent increases the number of active sites of adsorption present in the adsorbent [HAROON *et al.* 2016], as well as the residence time, therefore the diffusion of the ions is more effective, since the contact between the phases is more intimate [VILLABONA-ORTIZ *et al.* 2020].

**Table 1.** Analysis of variance (ANOVA) for nickel(II) adsorption

Source	Sum of squares	GI	F-ratio	p-value
A: temperature	5.40535	1	2.19	0.2358
B: particle size	19.1601	1	7.75	0.0488
C: bed height	36.4851	1	14.75	0.0311
AA	0.824487	1	0.33	0.6041
AB	1.39545	1	0.56	0.5071
AC	0.922112	1	0.37	0.5846
BB	2.99877	1	1.21	0.3512
BC	0.942819	1	0.38	0.5806
CC	12.9989	1	5.26	0.1057
Error total	7.41862	3	-	-
Total (corr.)	164.967	12	-	-

Source: own study.

Temperature is the evaluated factor with the least influence on the process, according to the variance analysis in Table 1. Its variation does not contribute significantly to the removal of the heavy metal. However, a slight increase in removal efficiency proportional to temperature is observed, which coincides with what is reported by SEIFPANAHI *et al.* [2017]. This may be because the temperature increase contributes to the speed of diffusion of the ions from the solution to the exposed surface of the biomaterial [AKPOMIE *et al.* 2018; ŠURÁNEK *et al.* 2021].

Table 1 shows the analysis of variance (ANOVA) performed at Statgraphics Centurion XVII. After partitioning the variability of the percentage of Ni(II) removal for each of the variables evaluated (particle size, temperature, and bed height), the significance of each effect was determined by comparing its average square with an estimate of the experimental error. In this case, two effects have a *p*-value lower than 0.05, bed height and particle size, so it is inferred that they have a direct influence on the process.

### BREAK CURVE MODELLING

The rupture curve, which studies the bed's behaviour over time, thus determining the saturation time and adsorption capacity [PATEL 2020; VILVANATHAN, SHANTHAKUMAR 2015] was evaluated for yam peel at the best condition found: 1.22 mm particle size, 70°C and 124 mm bed height, with a flow rate of 0.75 cm<sup>3</sup>·min<sup>-1</sup>

and initial concentration of 100 mg·dm<sup>-3</sup>, for 5 hours. The break curve data were adjusted to the models of Yoon–Nelson, Adams–Bohart, Dose–Response, and Thomas to analyse the processing time adsorption profile and describe a column's behaviour.

The Adams–Bohar model, represented in Equation (3), assumes that the rate of adsorption is proportional to the residual capacity of the solid and the concentration of the retained species, and is used to describe the initial part of the break curve [BOUCHERDOUD *et al.* 2021; SAADAT *et al.* 2016].

$$\frac{C}{C_o} = e^{k_{AB}C_i t - \frac{k_{AB}N_0 Z}{v}} \quad (3)$$

where: *C* = the concentration of solute in the liquid phase (mg·dm<sup>-3</sup>), *k*<sub>AB</sub> = the kinetic constant (dm<sup>3</sup>·mg<sup>-1</sup>·min<sup>-1</sup>), *t* = time (min), *N*<sub>0</sub> = the maximum volumetric sorption capacity (mg·dm<sup>-3</sup>), *Z* = the column filling height (cm), *v* = the linear flow rate (cm·min<sup>-1</sup>).

The Thomas model, described in Equation (4) is a derivation based on second-order kinetics and stipulates that biosorption is not limited by the chemical reaction but is controlled by the transfer of matter at the interface [CORRAL-ESCARCEGA *et al.* 2017; YUSUF *et al.* 2020].

$$\frac{C}{C_o} = \frac{1}{1 + e^{\left(\frac{k_{Th}}{Q}(q_{Th}w - C_i V_{ef}\right)}} \quad (4)$$

where: *k*<sub>Th</sub> = Thomas' speed constant (cm<sup>3</sup>·mg<sup>-1</sup>·min<sup>-1</sup>), *q*<sub>Th</sub> = the maximum concentration of solute in the solid phase (mg·g<sup>-1</sup>), *w* = mass of adsorbent (g), *V*<sub>ef</sub> = the cumulative throughput volume (l) of treated solution.

The Yoon–Nelson model assumes that the decrease rate in the probability of adsorption for each adsorbate molecule is proportional to the probability of adsorption of the adsorbate and the probability of advancement of the adsorbate into the adsorbent [YUSUF *et al.* 2020]. It is expressed by Equation (5):

$$\frac{C}{C_o} = \frac{1}{1 + e^{k_{YN}(\tau - t)}} \quad (5)$$

where: *k*<sub>YN</sub> = Yoon–Nelson's constant of proportionality (min<sup>-1</sup>), and *τ* = the time required to retain 50% of the initial adsorbate (min).

The Dose–Response model has been commonly used in pharmacology to describe different types of processes, and is currently being applied to describe bio-adsorption in columns, as summarised in Equation (6) [MOSCATELLO *et al.* 2018].

$$\frac{C}{C_o} = 1 - \frac{1}{1 + \left(\frac{C_o Q t}{q_0 X}\right)^a} \quad (6)$$

where: *a* = the model constant; *q*<sub>0</sub> = maximum solute concentration in the solid phase (mg·g<sup>-1</sup>); *X* = the amount of adsorbent in the column (g), *Q* = the flow rate (dm<sup>3</sup>·min<sup>-1</sup>).

The experimental data adjustment was fitted to the Adams–Bohart, Thomas, Yoon–Nelson, and Dose–Response models, as shown in Figure 3. The adjustment parameters of the models are shown in Table 2.



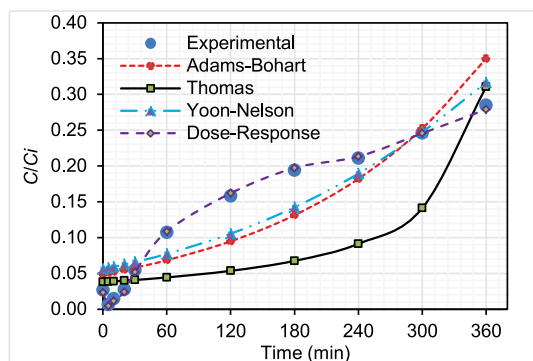


Fig. 3. Adjustment to break curve models; source: own study

Table 2. Adjustment parameters of the break curve models

Model	Parameter	Values
Thomas	$K_{Th}$ ( $\text{cm}^3 \cdot \text{min}^{-1} \cdot \text{mg}^{-1}$ )	0.6445
	$q_{Th}$ ( $\text{mg} \cdot \text{g}^{-1}$ )	15.3177
	SS	0.0059
	$R^2$	0.7707
Dose-Response	$q_{D-R}$ ( $\text{mg} \cdot \text{g}^{-1}$ )	1.1823
	$a$	19352.0616
	SS	1.1442E-5
	$R^2$	0.9996
Yoon-Nelson	$K_{Y-N}$ ( $\text{min}^{-1}$ )	0.0057
	$\tau$ (min)	494.9626
	SS	0.0014
	$R^2$	0.9296
Adams-Bohart	$K_{A-B}$ ( $\text{dm}^3 \cdot \text{mg}^{-1} \cdot \text{min}^{-1}$ )	5.4439E-5
	$N_0$ ( $\text{mg} \cdot \text{dm}^{-3}$ )	7056.3541
	SS	0.0192
	$R^2$	0.9062

Explanations:  $K_{Th}$  = Thomas' speed constant,  $q_{Th}$  = the maximum concentration of solute in the solid phase, SS = sum of squares,  $R^2$  = coefficient of correlation,  $q_{D-R}$  = maximum solute concentration in the solid phase,  $a$  = Dose-Response model constant,  $K_{Y-N}$  = Yoon-Nelson's constant of proportionality,  $\tau$  = the time required to retain 50% of the initial adsorbate,  $K_{A-B}$  = Adams-Bohart's constant of proportionality,  $N_0$  = the maximum volumetric sorption capacity

Source: own study

Figure 3 shows that the highest adsorption of metal ions occurs in the first instant of the process when making contact with the biomass due to the high availability of active sites in the unsaturated bio-adsorbent [MAHDI *et al.* 2018; YUSUF *et al.* 2020]. As the bed operation time elapsed, its efficiency gradually decreased due to the occupation of active sites. Therefore, the concentration of the effluent increased until the output concentration was 30% of the input concentration of 100  $\text{mg} \cdot \text{dm}^{-3}$  [ABDOLALI *et al.* 2017]. However, the adsorbent's total saturation is not reached in the column, so the trend of the break curve is upward after the contact time.

According to the sum of errors (SS) and the  $R^2$  presented in Table 2, it can be said the experimental data of Ni(II) removal on yam shells fit better to the Dose-Response model. Considering the industrial applications of adsorption, the identification of the advance time is vital since it defines the operational limit of the column. This fact is defined as the time interval in which the output concentration is higher than the threshold established, however such saturation was not reached in this study [YAHYA *et al.* 2020]. It was established that in the study time, the biomass can be used because they have a high capacity for heavy metal adsorption [MISHRA *et al.* 2016]. According to Equation (2),  $q_{total}$  of the column was established at  $16.1512 \text{ mg} \cdot \text{g}^{-1}$ ; thus, although the  $R^2$  value was calculated for the Dose-Response model, it was observed that the  $q_{D-R}$  determined for this model is significantly lower than the one obtained experimentally; in this sense, the model that is closest to the experimental values is the Thomas model, so it is assumed that the adsorption mechanism was a Langmuir type adsorption followed by a pseudo-second-order chemical sorption [LAVANYA *et al.* 2020; SRIVASTAVA *et al.* 2019]. The prediction of the break curve by the Thomas and Dose-Response model was previously reported using yersiniabactin as an adsorbent [MOSCATELLO *et al.* 2018], using red beans impregnated with magnetite nanoparticles [XAVIER *et al.* 2018], cocoa shells [VERA-CABEZAS *et al.* 2018], sugar cane bagasse [VERA *et al.* 2019] and K1AgNPs decorated MWCNTs nano-adsorbent [EGBOSIUBA *et al.* 2021].

## CONCLUSION

The conclusions from the present investigation are as follows: (i) The SEM-EDS analysis of yam shells shows a rough, heterogeneous, carbon, and oxygen-rich structure, featuring mesopores, suitable for the removal of heavy metals. (ii) Ni(II) removal efficiencies between 85.8 and 98.43%, showing the affinity of the bio-adsorbent for the metallic ion. (iii) The increase of the bed height and particle size favours the process obtaining a theoretical maximum removal for Ni(II) of 101.352% at 70°C, 1.22 mm of particle size and 124 mm of bed height; for a maximum capacity of adsorption in the bed of  $16.15 \text{ mg} \cdot \text{g}^{-1}$ . (iv) The Dose-Response model described the behaviour of the breakdown curve with  $R^2$  of 0.9996. (v) Yam shell is suggested as an alternative for removing Ni(II) ions present in an aqueous solution in a continuous system through bio-adsorption.

## ACKNOWLEDGMENTS

The authors are grateful to the University of Cartagena for the support in developing this research, laboratories, software, and time of the research professors.

## REFERENCES

- ABDOLALI A., NGO H.H., GUO W., ZHOU J.L., ZHANG J., LIANG S., CHANG S. W., NGUYEN D.D., LIU Y. 2017. Application of a breakthrough biosorbent for removing heavy metals from synthetic and real wastewaters in a lab-scale continuous fixed-bed column.

- Bioresource Technology. Vol. 229 p. 78–87. DOI 10.1016/j.biortech.2017.01.016.
- AFROZE S., SEN T.K. 2018. A review on heavy metal ions and dye adsorption from water by agricultural solid waste adsorbents. *Water, Air & Soil Pollution*. Vol. 229(7), 225. DOI 10.1007/s11270-018-3869-z.
- AKPOMIE K.G., ELUKE L.O., AJIWE V.I.E., ONYEMEZIRI A.C. 2018. Attenuation kinetics and desorption performance of *Artocarpus altilis* seed husk for Co (II), Pb (II) And Zn (II) ions. *Iranian Journal of Chemistry and Chemical Engineering*. Vol. 37. No. 3 p. 171–186.
- ANOOP KRISHNAN K., SREEJALEKSHMI K.G., BAIJU R.S. 2011. Nickel(II) adsorption onto biomass based activated carbon obtained from sugarcane bagasse pith. *Bioresource Technology*. Vol. 102 p. 10239–10247. DOI 10.1016/j.biortech.2011.08.069.
- APIRATIKUL R., CHU K.H. 2021. Improved fixed bed models for correlating asymmetric adsorption breakthrough curves. *Journal of Water Process Engineering*. Vol. 40, 101810. DOI 10.1016/j.jwpe.2020.101810.
- ASTM D6913-04 Standard test methods for particle-size distribution (gradation) of soils using sieve analysis [online]. American Society for Testing and Materials. [Access 10.10.2020]. Available at: <https://tienda.aenor.com/norma-astm-d6913-04-036631>
- BABARINDE A., OGUNDIPE K., SANGOSANYA K.T., AKINTOLA B.D., HASSAN A.-O.E. 2016. Comparative study on the biosorption of Pb(II), Cd(II) and Zn(II) using lemon grass (*Cymbopogon citratus*): Kinetics, isotherms and thermodynamics. *Chemistry International*. Vol. 2. No. 2 p. 89–102. DOI 10.5281/zenodo.1470602.
- BARQUILHA C.E.R., COSSICH E.S., TAVARES C.R.G., SILVA E.A. 2017. Biosorption of nickel(II) and copper(II) ions in batch and fixed-bed columns by free and immobilized marine algae *Sargassum* sp. *Journal of Cleaner Production*. Vol. 150 p. 58–64. DOI 10.1016/j.jclepro.2017.02.199.
- BATOOL F., AKBAR J., IQBAL S., NOREEN S., BUKHARI S.N.A. 2018. Study of isothermal, kinetic, and thermodynamic parameters for adsorption of cadmium: An overview of linear and nonlinear approach and error analysis. *Bioinorganic Chemistry and Applications*. Vol. 2018, 3463724. DOI 10.1155/2018/3463724.
- BIGDELOO M., TEYMOURIAN T., KOWSARI E., RAMAKRISHNA S., EHSANI A. 2021. Sustainability and circular economy of food wastes: Waste reduction strategies, higher recycling methods, and improved valorization. *Materials Circular Economy*. Vol. 3. No. 1, 3. DOI 10.1007/s42824-021-00017-3.
- BISWAS S., NAG S. 2021. Biomass-based adsorbents for heavy metal removal. In: *Green adsorbents to remove metals, dyes and boron from polluted water*. Eds. Inamuddin, M. Ahamed, E. Lichtfouse, A. Asiri. *Environmental Chemistry for a Sustainable World*. Vol. 49 p. 351–376. Springer, Cham. DOI 10.1007/978-3-030-47400-3\_14.
- BOUCHERDOUD A., KHERRROUB D.E., BESTANI B., BENDERDOUCHE N., DOUINAT O. 2021. Fixed-bed adsorption dynamics of methylene blue from aqueous solution using alginate-activated carbon composites adsorbents. *Algerian Journal of Environmental Science and Technology Month Edition*. Vol. 8. No. 1 p. 2329–2337.
- CHAO H.-P., CHUNG C.C., AILEEN N. 2014. Biosorption of heavy metals on *Citrus maxima* peel, passion fruit shell, and sugarcane bagasse in a fixed-bed column. *Journal of Industrial and Engineering Chemistry*. Vol. 20. No. 5 p. 3408–3414. DOI 10.1016/j.jiec.2013.12.027.
- CORRAL-ESCARCEGA M.C., RUIZ-GUTIÉRREZ M.G., QUINTERO-RAMOS A., MELÉNDEZ-PIZARRO C.O., LARDIZABAL-GUTIÉRREZ D., CAMPOS-VEÑE-GAS K. 2017. Use of biomass-derived from pecan nut husks (*Carya illinoensis*) for chromium removal from aqueous solutions. *Column Modeling and Adsorption Kinetics Studies*. *Revista Mexicana de Ingeniera Quimica*. Vol. 16. No. 3 p. 939–953.
- DAI Y., SUN Q., WANG W., LU L., LIU M., LI J., ZHANG Y. 2018. Utilizations of agricultural waste as adsorbent for the removal of contaminants: A review. *Chemosphere*. Vol. 211 p. 235–253. DOI 10.1016/j.chemosphere.2018.06.179.
- DEMIREL M., KAYAN B. 2012. Application of response surface methodology and central composite design for the optimization of textile dye degradation by wet air oxidation. *International Journal of Industrial Chemistry*. Vol. 3, 24 p. 1–10. DOI 10.1186/2228-5547-3-24.
- DENG Y., HUANG S., DONG C., MENG Z., WANG X. 2020. Competitive adsorption behaviour and mechanisms of cadmium, nickel and ammonium from aqueous solution by fresh and ageing rice straw biochars. *Bioresource Technology*. Vol. 303, 122853. DOI 10.1016/j.biortech.2020.122853.
- DENG Y., HUANG S., LAIRD D.A., WANG X., DONG C. 2018. Quantitative mechanisms of cadmium adsorption on rice straw- and swine manure-derived biochars. *Environmental Science and Pollution Research*. Vol. 25. No. 32 p. 32418–32432. DOI 10.1007/s11356-018-2991-1.
- EGBOSIUBA T.C., ABDULKAREEM A.S., KOVO A.S., AFOLABI E.A., TIJANI J.O., BANKOLE M.T., BO S., ROOS W.D. 2021. Adsorption of Cr(VI), Ni (II), Fe(II) and Cd(II) ions by KIAgNPs decorated MWCNTs in a batch and fixed bed process. *Scientific Reports*. Vol. 11. No. 1, 75. DOI 10.1038/s41598-020-79857-z.
- HAROON H., ASHFAQ T., GARDAZI S.M.H., SHERAZI T.A., ALI M., RASHID N., BILAL M. 2016. Equilibrium kinetic and thermodynamic studies of Cr(VI) adsorption onto a novel adsorbent of eucalyptus camaldulensis waste: Batch and column reactors. *Korean Journal of Chemical Engineering*. Vol. 33. No. 10 p. 2898–2907. DOI 10.1007/s11814-016-0160-0.
- HERRERA-BARROS A., BITAR-CASTRO N., VILLABONA-ORTÍZ Á., TEJADA-TOVAR C., GONZÁLEZ-DELGADO Á.D. 2020. Nickel adsorption from aqueous solution using lemon peel biomass chemically modified with TiO<sub>2</sub> nanoparticles. *Sustainable Chemistry and Pharmacy*. Vol. 17, 100299. DOI 10.1016/j.scp.2020.100299.
- LARA J., TEJADA-TOVAR C., VILLABONA-ORTÍZ A., ARRIETA A. 2016. Adsorption of lead and cadmium in continuous of fixed bed on cocoa waste. *Revista ION*. Vol. 29. No. 2 p. 111–122. DOI 10.18273/revion.v29n2-2016009.
- LAVANYA R., GOMATHI T., NITHYA R., SUDHA P.N. 2020. Fixed-bed column adsorption studies of lead (II) from aqueous solution using Chitosan-G-Maleic Anhydride-G-Methacrylic Acidcopolymer. *Journal of Science and Technology*. Vol. 5. No. 4 p. 316–334. DOI 10.46243/jst.2020.v5.i4.pp316-334.
- LIANG X., WEI G., XIONG J., TAN F., HE H., QU C., ..., JING Z. 2017. Adsorption isotherm, mechanism, and geometry of Pb(II) on magnetites substituted with transition metals. *Chemical Geology*. Vol. 470 p. 132–140. DOI 10.1016/j.chemgeo.2017.09.003.
- MAHARANA M., MANNA M., SARDAR M., SEN S. 2021. Heavy metal removal by low-cost adsorbents. In: *Green adsorbents to remove metals, dyes and boron from polluted water*. Eds. Inamuddin, M.I. Ahamed, E. Lichtfouse, A.M. Asiri. Cham. Springer p. 245–272. DOI 10.1007/978-3-030-47400-3\_10.
- MAHDI Z., YU Q.J., EL HANANDEH A. 2018. Investigation of the kinetics and mechanisms of nickel and copper ions adsorption from aqueous solutions by date seed derived biochar. *Journal of Environmental Chemical Engineering*. Vol. 6. No. 1 p. 1171–1181. DOI 10.1016/j.jece.2018.01.021.

- MALIK R., BHASKARAN M., LATA S. 2021. Heavy metal removal from wastewater using adsorbents. In: Water pollution and remediation: Heavy metals. Eds. Inamuddin, M.I. Ahamed, E. Lichtfouse p. 441–469. Cham. Springer. DOI 10.1007/978-3-030-52421-0\_13.
- MANJULADEVI M., ANITHA R., MANONMANI S. 2018. Kinetic study on adsorption of Cr (VI), Ni (II), Cd (II) and Pb (II) ions from aqueous solutions using activated carbon prepared from *Cucumis melo* peel. Applied Water Science. Vol. 8. No. 1, 36. DOI 10.1007/s13201-018-0674-1.
- MARTÍN-LARA, M.Á., TRUJILLO MIRANDA M.C., RONDA GÁLVEZ A., PÉREZ MUÑOZ A., CALERO DE HOCES M. 2017. Valorization of olive stone as adsorbent of chromium(VI): Comparison between laboratory- and pilot-scale fixed-bed columns. International Journal of Environmental Science and Technology. Vol. 14. No. 12 p. 2661–2674. DOI 10.1007/s13762-017-1345-8.
- MISHRA A., TRIPATHI B.D., RAI A.K. 2016. Packed-bed column biosorption of chromium (VI) and nickel (II) onto fenton modified hydrilla verticillata dried biomass. Ecotoxicology and Environmental Safety. Vol. 132 p. 420–428. DOI 10.1016/j.ecoenv.2016.06.026.
- MOINO B.P., COSTA C.S.D., DA SILVA M.G.C., VIEIRA M.G.A. 2017. Removal of nickel ions on residue of alginate extraction from *Sargassum filipendula* seaweed in packed bed. Canadian Journal of Chemical Engineering. Vol. 95. No. 11 p. 2120–2128. DOI 10.1002/cjce.22859.
- MOSCATELLO N., SWAYAMBHU G., JONES C.H., XU J., DAI N., PFEIFER B.A. 2018. Continuous removal of copper, magnesium, and nickel from industrial wastewater utilizing the natural product yersiniabactin immobilized within a packed-bed column. Chemical Engineering Journal. Vol. 343 p. 173–179. DOI 10.1016/j.cej.2018.02.093.
- NAGHIZADEH A., GHASEMI F., DERAKHSHANI E., SHAHABI H. 2017. Thermodynamic, kinetic and isotherm studies of sulfate removal from aqueous solutions by graphene and graphite nanoparticles. Desalination and Water Treatment. Vol. 80 p. 247–254. DOI 10.5004/dwt.2017.20891.
- NITHYA K., SATHISH A., SENTHIL KUMAR P. 2020. Packed bed column optimization and modeling studies for removal of chromium ions using chemically modified *Lantana camara* adsorbent. Journal of Water Process Engineering. Vol. 33, 101069. DOI 10.1016/j.jwpe.2019.101069.
- PATEL H. 2020. Batch and continuous fixed bed adsorption of heavy metals removal using activated charcoal from neem (*Azadirachta indica*) leaf powder. Scientific Reports. Vol. 10. No. 1, 16895. DOI 10.1038/s41598-020-72583-6.
- PRIYANTHA N., LIM L.B.L., MALLIKARATHNA S., KULASOORIYA T.P.K. 2019. Enhanced removal of Ni(II) by acetic acid-modified peat. Desalination and Water Treatment. Vol. 137 p. 162–173. DOI 10.5004/dwt.2019.23213.
- RAULINO G.S.C., VIDAL C.B., LIMA A.C.A., MELO D.Q., OLIVEIRA J.T., NASCIMENTO R.F. 2014. Treatment influence on green coconut shells for removal of metal ions: pilot-scale fixed-bed column. Environmental Technology (United Kingdom). Vol. 35. No. 14 p. 1711–1720. DOI 10.1080/09593330.2014.880747.
- RESKE G.D., DA ROSA B.C., VISIOLI L.J., DOTTO G.L., DE CASTILHOS F. 2020. Intensification of Ni(II) adsorption in a fixed bed column through subcritical conditions. Chemical Engineering and Processing – Process Intensification. Vol. 149, 107863. DOI 10.1016/j.cep.2020.107863.
- SAADAT S., HEKMATZADEH A.A., JASHNI A.K. 2016. Mathematical modeling of the Ni(II) removal from aqueous solutions onto pre-treated rice husk in fixed-bed columns: A comparison. Desalination and Water Treatment. Vol. 57. No. 36 p. 16907–16918. DOI 10.1080/19443994.2015.1087877.
- SABIR A., ALTAFF F., BATOOL R., SHAFIQ M., KHAN R.U., JACOB K.I. 2021. Agricultural waste adsorbents for heavy metal removal. In: Green adsorbents to remove metals, dyes and boron from polluted water. Eds. Inamuddin, M.I. Ahamed, E. Lichtfouse, A.M. Asiri. Cham. Springer p. 195–228. DOI 10.1007/978-3-030-47400-3\_8.
- SEIFPANAHI K.S., ARDEJANI F.D., BADI K., OLYA M.E. 2017. Preparation and characterization of novel nano-mineral for the removal of several heavy metals from aqueous solution: Batch and continuous systems. Arabian Journal of Chemistry. Vol. 10. No. 2 p. 3108–3127. DOI 10.1016/j.arabjc.2013.12.001.
- SRIVASTAVA S., AGRAWAL S.B., MONDAL M.K. 2019. Fixed bed column adsorption of Cr(VI) from aqueous solution using nanosorbents derived from magnetite impregnated *Phaseolus vulgaris* husk. Environmental Progress and Sustainable Energy. Vol. 38. No. s1 p. S68–S76. DOI 10.1002/ep.12918.
- ŠURÁNEK M., MELICHOVÁ Z., KUREKOVÁ V., KLJAJEVIĆ L., NENADOVIĆ S. 2021. Removal of nickel from aqueous solutions by natural bentonites from Slovakia. Materials. Vol. 14 No. 2, 282. DOI 10.3390/ma14020282.
- TEJADA-TOVAR C., VILLABONA-ORTÍZ A., RAMÍREZ-VÁSQUEZ P. 2020. Valorización de residuos de la obtención de almidón de ñame espino para su uso como bioadsorbente en la remoción de Cromo (VI) y Níquel (II) [Waste valorization of starch obtained from hawthorn yam as bioadsorbent on chromium (VI) and nickel (II) removal]. INGE CUC. Vol. 16. No. 1 p. 1–10. DOI 10.17981/ingecuc.16.1.2020.02.
- TEJADA-TOVAR C., VILLABONA-ORTÍZ A., ROMERO-MURILLO L., FLOREZ-MADRIGAL G., ACEVEDO D. 2018. Design of a modular filtration-adsorption system for removal of methylene blue and turbidity using activated carbons and a sand-gravel-anthracite filter. International Journal of ChemTech Research. Vol. 11. No. 05 p. 249–264. DOI 10.20902/ijctr.2018.110528.
- TOBÓN-OROZCO D., VASCO CORREA C.A. 2021. Water environmental regulation in Colombia. Kairós, Revista De Ciencias Económicas, Jurídicas Y Administrativas. Vol. 4. No. 6 p. 82–96. DOI 10.37135/kai.03.06.06.
- VERA L.M., BERMEJO D., UGUÑA M.F., GARCIA N., FLORES M., GONZÁLEZ E. 2019. Fixed bed column modeling of lead(II) and cadmium(II) ions biosorption on sugarcane bagasse. Environmental Engineering Research. Vol. 24. No. 1 p. 31–37. DOI 10.4491/eer.2018.042.
- VERA-CABEZAS, L., BERMEJO D., ROSAS M.U., ALVEAR N.G., ZAMORA M.F., BRAZALES D. 2018. Biosorption of Pb (II) and Cd (II) in fixed bed columns with cocoa shell. Afinidad. Vol. 75. No. 581 p. 16–22.
- VILLABONA-ORTIZ Á., TEJADA-TOVAR C., RUIZ-PATERNINA E., FRÍAS-GONZÁLEZ J.D., BLANCO-GARCÍA G.D. 2020. Optimization of the effect of temperature and bed height on Cr (VI) bioadsorption in continuous system. Revista Facultad de Ingeniería. Vol. 29. No. 54, e10477.
- VILVANATHAN S., SHANTHAKUMAR S. 2015. Column adsorption studies on nickel and cobalt removal from aqueous solution using native and biochar form of *Tectona grandis*. Environmental Progress & Sustainable Energy. Vol. 35(3) p. 809–814. DOI 10.1002/ep.12567.
- WU S., WANG C., JIN Y., ZHOU G., ZHANG L., YU P., SUN L. 2021. Green synthesis of reusable super-paramagnetic diatomite for aqueous nickel (II) removal. Journal of Colloid and Interface Science. Vol. 582 p. 1179–1190. DOI 10.1016/j.jcis.2020.08.119.
- XAVIER A.L.P., HERRERA ADARME O.F., FURTADO L.M., FERREIRA G.M.D., MENDES DA SILVA L.H., GIL L.F., GURGEL L.V.A. 2018. Modeling

adsorption of copper(II), cobalt(II) and nickel(II) metal ions from aqueous solution onto a new carboxylated sugarcane bagasse. Part II: Optimization of monocomponent fixed-bed column adsorption. *Journal of Colloid and Interface Science*. Vol. 516 p. 431–445. DOI [10.1016/j.jcis.2018.01.068](https://doi.org/10.1016/j.jcis.2018.01.068).

YAHYA M.D., IHEJIRIKA C.V., IYAKA Y.A., GARBA U., OLUGBENGA A.G. 2020. Continuous sorption of chromium ions from simulated effluents using citric acid modified sweet potato peels. *Nigerian Journal of Technological Development*. Vol. 17. No. 1 p. 47–54. DOI [10.4314/njtd.v17i1.7](https://doi.org/10.4314/njtd.v17i1.7).

YU G., WANG X., LIU J., JIANG P., YOU S., DING N., GUO Q., LIN F. 2021. Applications of nanomaterials for heavy metal removal from water and soil: A review. *Sustainability*. Vol. 13. No. 2, 713. DOI [10.3390/su13020713](https://doi.org/10.3390/su13020713).

YUSUF M., SONG K., LI L. 2020. Fixed bed column and artificial neural network model to predict heavy metals adsorption dynamic on surfactant decorated graphene. *Colloids and Surfaces A: Physicochemical and Engineering Aspects*. Vol. 585, 124076. DOI [10.1016/j.colsurfa.2019.124076](https://doi.org/10.1016/j.colsurfa.2019.124076).